Geofísica Internacional (2011) 50-3: 279-293

Original paper

Factors influencing the fault displacement-length relationship: an example from the Cantarell oilfield, Gulf of Mexico

Xu Shunshan*, Ángel Francisco Nieto-Samaniego, Luis Germán Velasquillo-Martínez, José Manuel Grajales-Nishimura, Gustavo Murillo-Muñetón and Jesús García-Hernández

Received: June 24, 2010; accepted: March 9, 2011; published on line: June 30, 2011

Resumen

Asumiendo que la relación entre máxima longitud y máximo desplazamiento en las fallas es lineal, investigamos los efectos de considerar distintos componentes del desplazamiento, del nivel de observación, y la presencia de enlace de fallas. Para ello usamos datos de las fallas normales del bloque Akal, en el campo petrolero de Cantarell, localizado en el Golfo de México frente a las costas de Campeche. Los datos que se utilizaron fueron tomados de mapas de contornos de cuatro horizontes diferentes. Los resultados obtenidos pueden resumirse de la manera siguiente: (1) el desplazamiento al echado es mejor que el desplazamiento vertical para el análisis de la relación D-L; (2) utilizando fallas que muestran sus dos terminaciones se logran mejores coeficientes de correlación lineal entre D y L, que utilizando fallas con una sola o ninguna terminación; (3) los coeficientes de correlación (R_L^2) obtenidos para las gráficas D-L en cada horizonte son distintos, lo que indica que los valores de (R_L^2) son dependientes del nivel de observación.

Palabras clave: falla, desplazamiento de falla, longitud de falla, enlace de falla, México.

Abstract

Assuming a linear relationship between maximum length (*L*) and maximum fault displacement (*D*) we investigate the effects of displacement component measured, observation level, and fault linkage by using data from the normal faults of the Akal block of the Cantarell oilfield in the southern Gulf of Mexico (off Campeche). The data are measured from structural contour maps at four different horizons. The summarized results are: (1) dip displacement is better than vertical displacement to analyze the *D-L* relationship; (2) data from two-tip faults produce higher correlation coefficients (R_L^2) for linear regression between *D* and *L* than one-tip faults; (3) The correlation coefficients (R_L^2) are different for each analyzed horizons, suggesting that the value of R_L^2 is dependent on the observed level.

Key words: fault, displacement, length, sampling, linkage, Mexico.

Xu Shunshan*
Centro de Geociencias
Universidad Nacional Autónoma de México
Apartado Postal 1-742, 76001
Querétaro, Qro., México.
*Corresponding author:sxu@dragon.geociencias.unam.mx

A. F. Nieto-Samaniego
Centro de Geociencias
Universidad Nacional Autónoma de México
Apartado Postal 1-742, 76001
Querétaro, Qro., México.

L.G. Velasquillo-Martínez
Instituto Mexicano del Petróleo
Eje Central Lázaro Cárdenas No. 152
Col. San Bartolo Atepehuacan, 07730,
México D.F., México.

J. M. Grajales-Nishimura
Instituto Mexicano del Petróleo
Eje Central Lázaro Cárdenas No. 152
Col. San Bartolo Atepehuacan, 07730,
México D.F., México.

G. Murillo-Muñetón
Instituto Mexicano del Petróleo
Eje Central Lázaro Cárdenas No. 152
Col. San Bartolo Atepehuacan, 07730,
México D.F., México.

J. García-Hernández
Petróleos Mexicanos Exploración
y Producción Región Marina NE,
Activo Cantarell (PEP-RMNE).

Introduction

The relationship between the maximum displacement (D) and fault length (L) of faults is commonly written as a power law:

$$D = cL^n , \quad (1)$$

where c is a constant related to material properties. Whether a universal value of n exists is a debated issue. The published values of n range from 0.5 to 2.0 (e.g. Watterson, 1986; Walsh and Watterson, 1988; Marrett and Allmendinger, 1991; Bonnet *et al.*, 2001; Mazzoli *et al.*, 2005). Published data show that the relationship of maximum displacement to fault trace length is linear for tectonic environments with uniform mechanical properties (Cowie and Scholz, 1992; Dawers *et al.*, 1993; Xu *et al.*, 1998; Xu *et al.*, 2006; Schultz *et al.*, 2008). Many researchers accept that $n = 1$ on that condition.

The value of n is important for explaining the mechanism of fault growth and in a more practical sense, for estimating D from measurements of L or vice versa. For a given value of n, both maximum displacement and length increase with fault growth (Figure 1a). However, the gradients are different depending on the value of n. For $n = 1$, the rate of increase for both D and L remains constant during the growth of the fault. For $n < 1$, at the initial stage (part A in Figure 1a), the gradient of D is steeper than that of L, at a higher stage (part B in Figure 1a) the gradient of D is nearly equal to that of L, and in the final stage (part C in Figure 1a), the gradient of D is smaller than that of L. Similarly, for $n > 1$, at first stage the gradient of D is than that of L, at second stage (part B in Figure 1a) the gradient of D is nearly equal to that for L, whereas at the final stage the gradient of increase for D is higher than that for L (Figure 1a).

The objective of this paper is to investigate how sampling influences the measured fault parameters, in order to determine better sampling conditions. The fault plane is considered to have elliptical shape (Walsh and Watterson, 1987). The dimension along the slip direction is shorter than that nomal to the slip direction (Figures 1b, 1c, 1d). Thus, for normal and reverse faults, the dip dimension is shorter than the strike dimension (Figures 1b, 1c). For strike-slip faults, the strike dimension is longer than the dip dimension (Figure 1d). In our study area, the faults are normal faults similar to the ellipse in Figure 1b. For simplicity we assume that $n = 1$, and we analyze an example from the Cantarell oilfield in the southern Gulf of Mexico. The parameters considered in the study area were fault displacement components, fault interaction, and observation level.

Geological background

The Cantarell oilfield is located in the Gulf of Mexico, in the southern part of the North American Plate (Fig. 2a). The tectonics of the Gulf of Mexico is controlled by the interactions of the Caribbean, North America and Cocos plates at least for the last 74 Ma (Whitman *et al*., 1983). The Middle America trench marks the location of north-eastward subduction of the Cocos plate under the North American and Caribbean plates (LeFevre and McNally, 1985). In Campeche

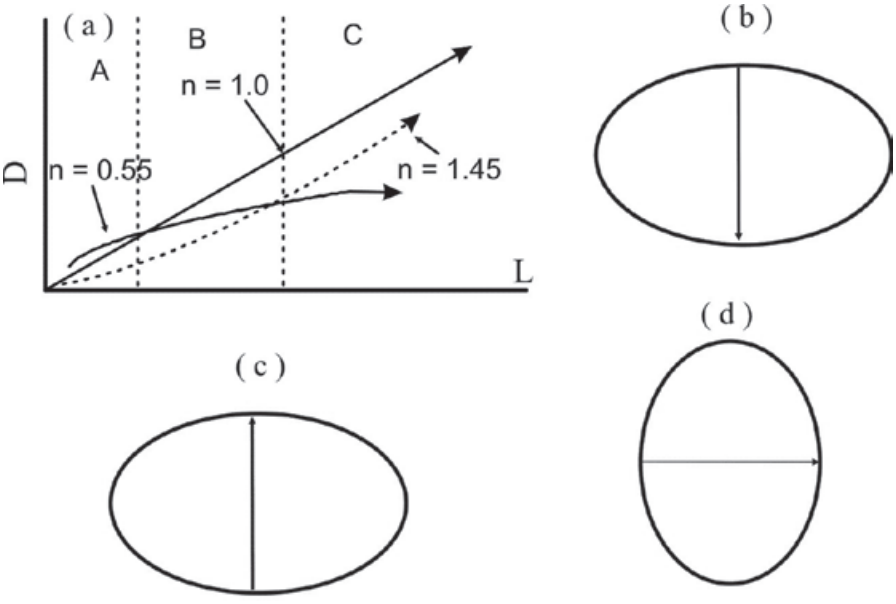

Figure 1. (a) Growth trend of fault from equation $D = cL^n$. The arrow indicates the growth direction. (b), (c), and (d) illustrate the fault shape for normal fault, reverse fault and strike-slip fault, respectively. The arrow indicates slip direction.

Bay (Figure 2) three main superimposed tectonic regimes are recorded: extensional, compressional, and extensional (Angeles-Aquino *et al*., 1994). The first period initiated in Middle Jurassic, and is related to the opening of the Gulf of Mexico. During this regime NW-SE faulting was dominant. The subsequent compressional regime took place in Middle Miocene. It was related to a northeast principal stress which often formed overturned anticlines. The last extensional regime extended through Middle and Late Miocene and has a Middle Miocene shaly horizon as detachment surface. During the last two regimes a salt tectonics occurred in the area, overprinting structures and disturbing the regional stress field.

Similarly, three main episodes of deformation occurred in the Cantarell oilfield (Mitra *et al*., 2005). First, extension during Jurassic to Early Cretaceous produced normal faults that mainly affected Tithonian, Kimmeridgian, and Lower Cretaceous units. Second, compression in Miocene produced the NW trending Cantarell thrust system. The Sihil thrust fault separates the allochthonous and autochthonous blocks (Figures 2b, 2c). Third, there was Pliocene to Holocene extension; during this phase of deformation several preexisting Jurassic normal faults were reactivated and new NS to NW trending normal faults were formed. The structural style in the Cantarell complex has been shaped by three major tectonic phases. The Akal anticline is a

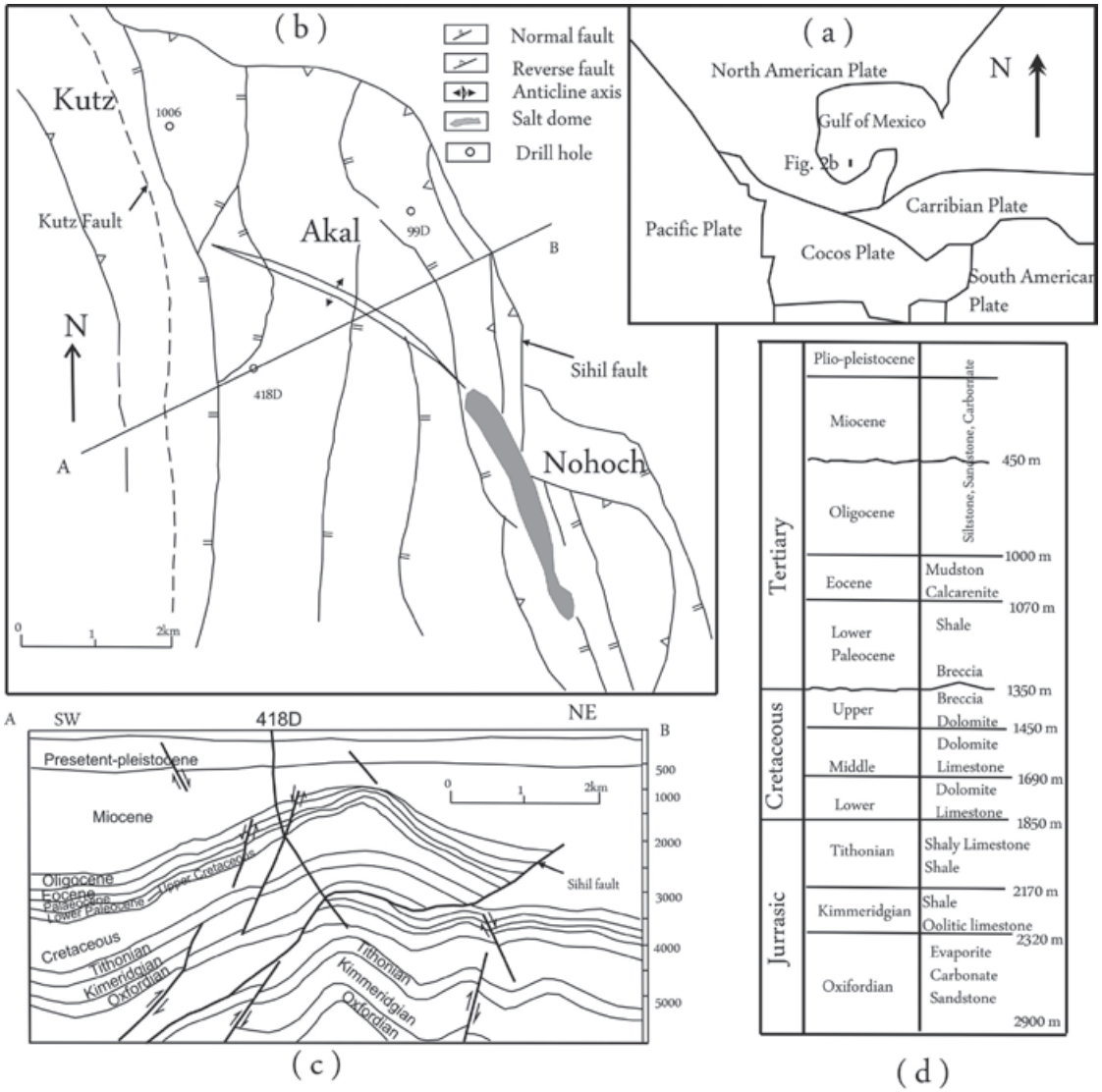

Figure 2. (a) Simplified plate map showing the location of the Gulf of Mexico and Cantarell oilfield. (b) Structural sketch of Cantarell oilfield. (c) Typical cross section in the studied area. (d) Integrated stratigraphic column of the Cantarell oilfield.

structure associated with the reverse fault belt. The anticline trends SE-NW and slightly plunges to southeast. The interpreted seismic section shows that the northeastern limb of Akal anticline is steeper than the southwestern limb (Aquino-Lopez, 1999).

We select the Akal block of the Cantarell oilfield in the southern Gulf of Mexico (offshore Campeche) as a case study (Figure 2b). The stratigraphic records in this oil field are shown in Figure 2d (PEMEX-Exploración Producción, 1999; Murillo-Muñetón *et al*., 2002). The main unit include: Callovian salt, Oxfordian siliciclastic strata and evaporites, Kimmeridgian carbonates and terrigenous rocks, Tithonian silty and bituminous limestone, Cretaceous dolomites, and dolomitized breccias in the Cretaceous-Tertiary boundary and Lower Paleocene. The Tertiary system includes siltstone, sandstone and carbonate rocks.

Previous studies have been published regarding structural features of the Cantarell oilfield (e.g., Santiago and Baro, 1992; PEMEX-Exploración Producción, 1999; Mitra *et al.*, 2005). The azimuth of the crest of the Akal anticline is about 300°NW. The fold is a SE-plunging fold. The angle between limbs of the fold is intermediate. The faults in the Akal block are normal faults, but the observed slickenside striations in minor faults from core samples are generally not along the fault dips (Xu *et al.*, 2004), implying that the faults have a strike component of displacement. Based on the evident strike component of displacement on fault planes, Pacheco (2002) suggested that these faults were formed by simple shear related to the movement of a larger fault (fault A in Figure 3a). However, recent interpretation of geophysical data suggest that Cantarell is a fold-thrust belt and a duplex structure, related to the Sihil thrust in Figure 2a and Figure 3 (Mitra *et al.*, 2005).

We use structural contour maps to measure fault displacements and fault trace lengths. Four structural maps of scale 1:50,000 were selected (Figure 3): the dolomitized breccias at the top of the Cretaceous/Tertiary boundary (T1, Figure 3a), the top of the Lower Cretaceous (T2, Figure 3b), the top of the Tithonian (T3, Figure 3c), and the top of the Kimmeridgian (T4, Figure 3d). We measured fault displacements with the method proposed by Xu *et al.* (2004).

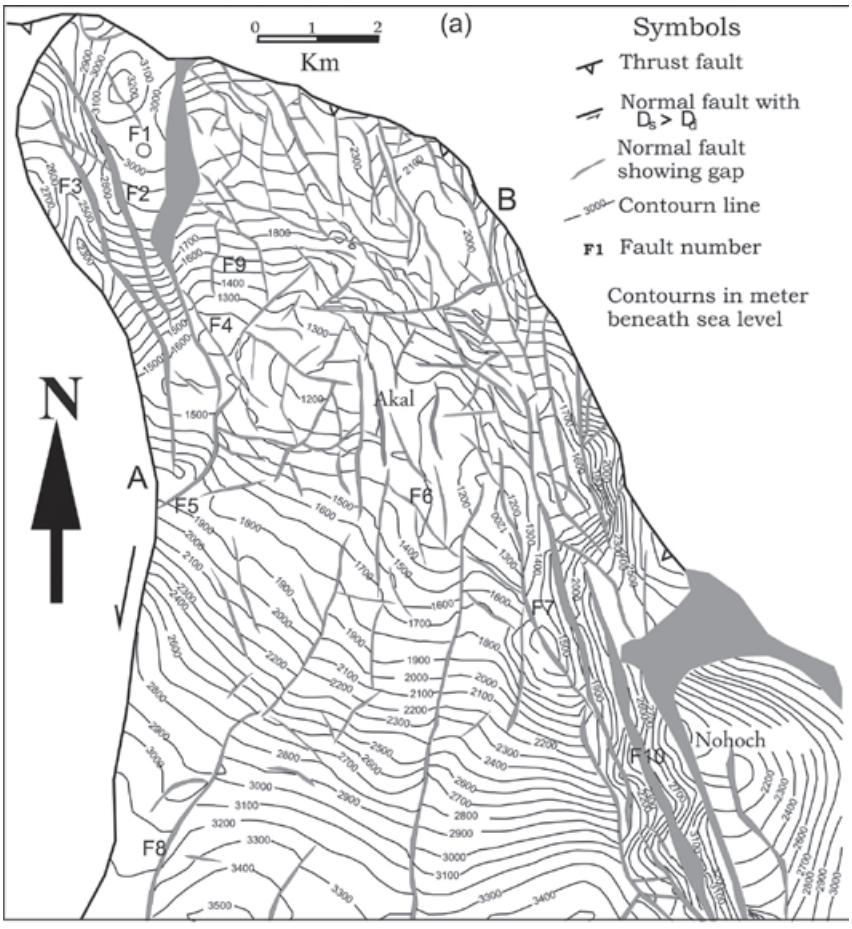

Figure 3. Structural contour maps in the Akal bock of Cantarell oilfield offshore Mexico. Contours are in meters. (a) The top of the Cretaceous-Tertiary carbonate breccia (T1). (b) The top of Lower Cretaceous (T2). (c) The top of Tithonian (T3). (d) The top of Kimmeridgian (T4). A and B are major faults in the Cantarell Oilfield.

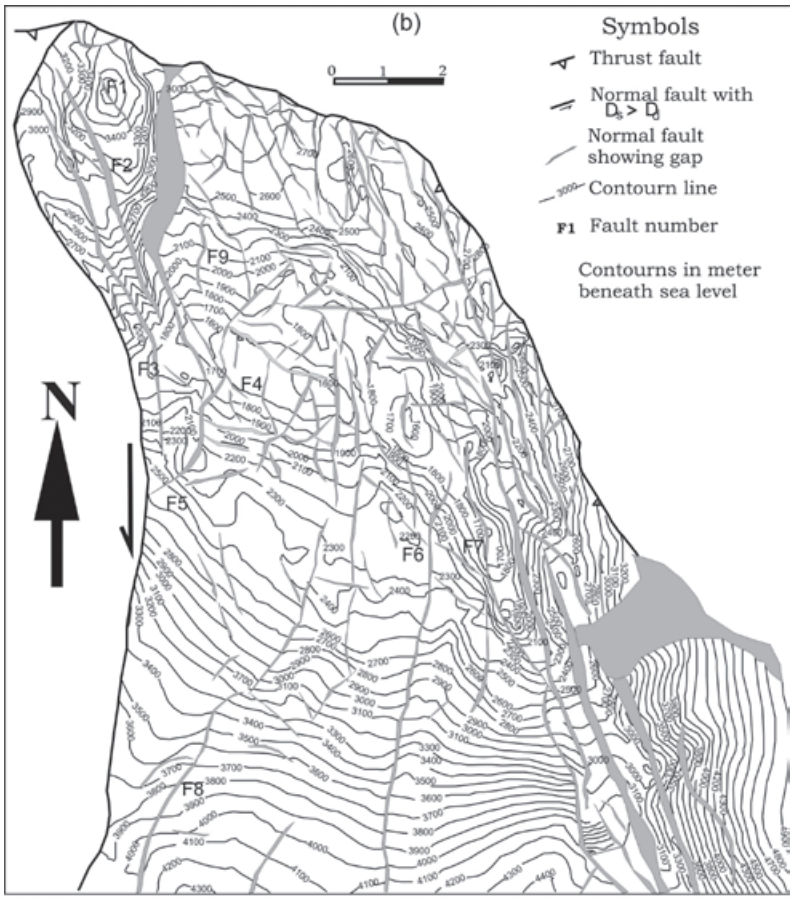

Figure 3b.

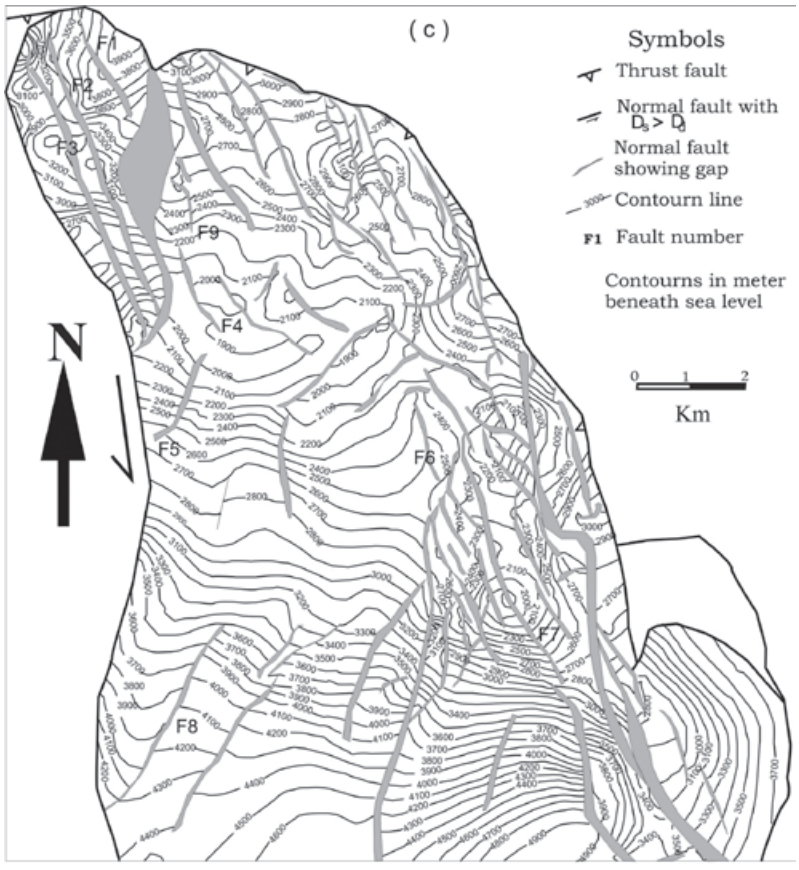

Figure 3c.

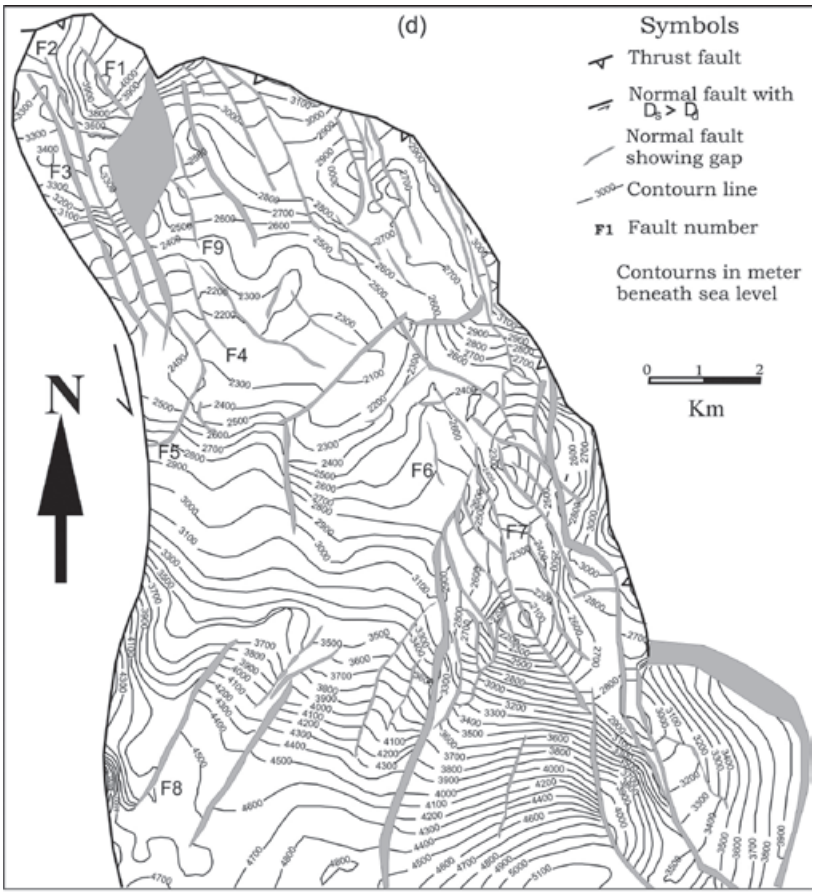

Figure 3d.

Correlation coefficients for linear and power-law relationship between *D* and *L*

As mentioned above, the relationship between *D* and *L* is debated (e.g., Bonnet *et al.*, 2001). Some published datasets show a power-law relationship (e.g. Marrett and Allmendinger, 1991), whereas other datasets express a linear relationship (e.g. Dawers *et al.*, 1993). In a previous study the maximum displacement and length of fault was shown to obey linear relationship (Xu *et al.*, 2006). In this work, we had analyzed data of two-tip faults to compare the correlation coefficients of linear and power-law regressions analysis between *D* and *L*. The results (Figure 4) showed that the coefficients for both linear and power-law relationships are not large. In most cases the coefficients for linear regression are larger than those for power-law analysis; this was also observed for datasets combined from four horizons (Figure 4e). These results indicate that a linear relationship between *D* and *L* may be better, although there is scatter in the *D*-*L* graphs in the case study of the Akal block. In the following, we document the reasons for low coefficients of the displacement-length linear relationship.

Effect of displacement component

What displacement components should be used to analyze the *D*-*L* relationship depends on the fault type. According to Walsh and Watterson (1988), fault displacement refers to the displacement accumulated through the whole active period of the fault. Thus the total true displacement should be used to analyze the relationship between fault displacement and trace length: in the case of a pure dip-slip normal fault the true displacement should be measured along the fault dip. However, in practice, the true displacements are difficult to obtain.

Displacement also represents the variation in position of a marker displaced by the fault movement (Tearpock and Bishchke, 2003). The throw or the strike component of displacement may be used to analyze the relationship between fault displacement and trace length (e.g. Dawers *et al.*, 1993; Peacock, 1991; 2002; Acocella and Neri, 2005).

Here we use dip displacement and vertical displacement of faults for each map or level (Figure 5). In our study area, the normal faults

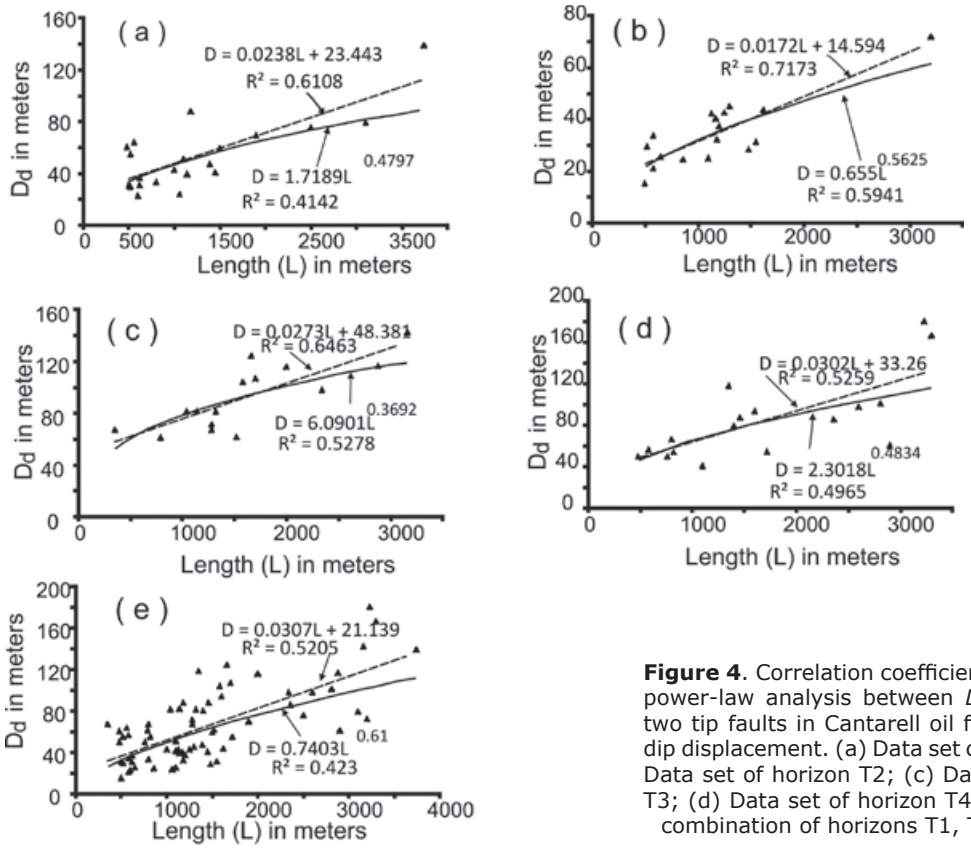

Figure 4. Correlation coefficients for linear and power-law analysis between D_d and L for the two tip faults in Cantarell oil field, where D_d is dip displacement. (a) Data set of horizon T1; (b) Data set of horizon T2; (c) Data set of horizon T3; (d) Data set of horizon T4; (e) Data set of combination of horizons T1, T2, T3, and T4.

have minor strike components of displacement, so the dip slip is close to the total displacement. Assuming that the faults are pure dip-slip faults, the dip displacement is a good proxy of the total displacement. By comparing respectively Figure 5a and Figure 5b, Figure 5c and Figure 5d, Figure 5e and Figure 5f, Figure 5g and Figure 5h, we can see that the correlation coefficients from dip displacement are larger than for vertical displacement, indicating that dip displacement produces less deviation from linear D-L relationship.

Effect of fault interaction

Displacement is zero at fault tips and commonly reaches a maximum near the center (Walsh and Watterson, 1987; Dawers *et al.*, 1993). Therefore, two initially isolated segments have a local displacement minimum located in the relay zone with two maximum near the center of each fault segment (Ellis and Dunlap, 1988; Caskey *et al.*, 1996; Soliva and Benedicto, 2005). After segment linkage, the maximum displacement is not located near the center of the new larger fault (Willemse, 1997). In the case of soft linkage, the displacement gradient decreases near the relay zone. If we measure the maximum displacement from the center of the linked fault, the maximum displacement will be underestimated.

For comparison, we analyzed three types of datasets for each level or map. One type of data set is from two-tip faults, which do not cut other faults or are not cut by other faults. Another type of data set corresponds to the one-tip or no-tip faults, which have branching faults or are branching faults themselves. The third type of data set is a mixture data set, including all kinds of faults. The idea of "restricted fault" relates to observer criteria because soft linkage may exist when the distance separating two segments is approximately an order of magnitude less than the individual segment length (Walsh and Watterson, 1991). From observation an isolated fault may connect with other faults (Childs *et al.*, 1995; Mansfield and Cartwright, 2001; Willemse, 1997; Davis *et al.*, 2005). For example, fault 6 is a no-tip fault when observed from the top of T1 (Figure 3a), a best two-tip fault when observed from the top of T3 and T4 (Figures 3c, 3d).

Two results are obtained by analyzing the data in the study area. First, in all cases there is a high scatter in the *D-L* graphs, the correlation coefficients are not larger than 0.75 (Figure 6). Second, the correlation coefficients from linear analysis for the two-tip faults are larger than 0.55, which indicates a possible linear relationship between *D* and *L*. The correlation coefficients for the one-tip or no-tip faults are smaller than 0.5,

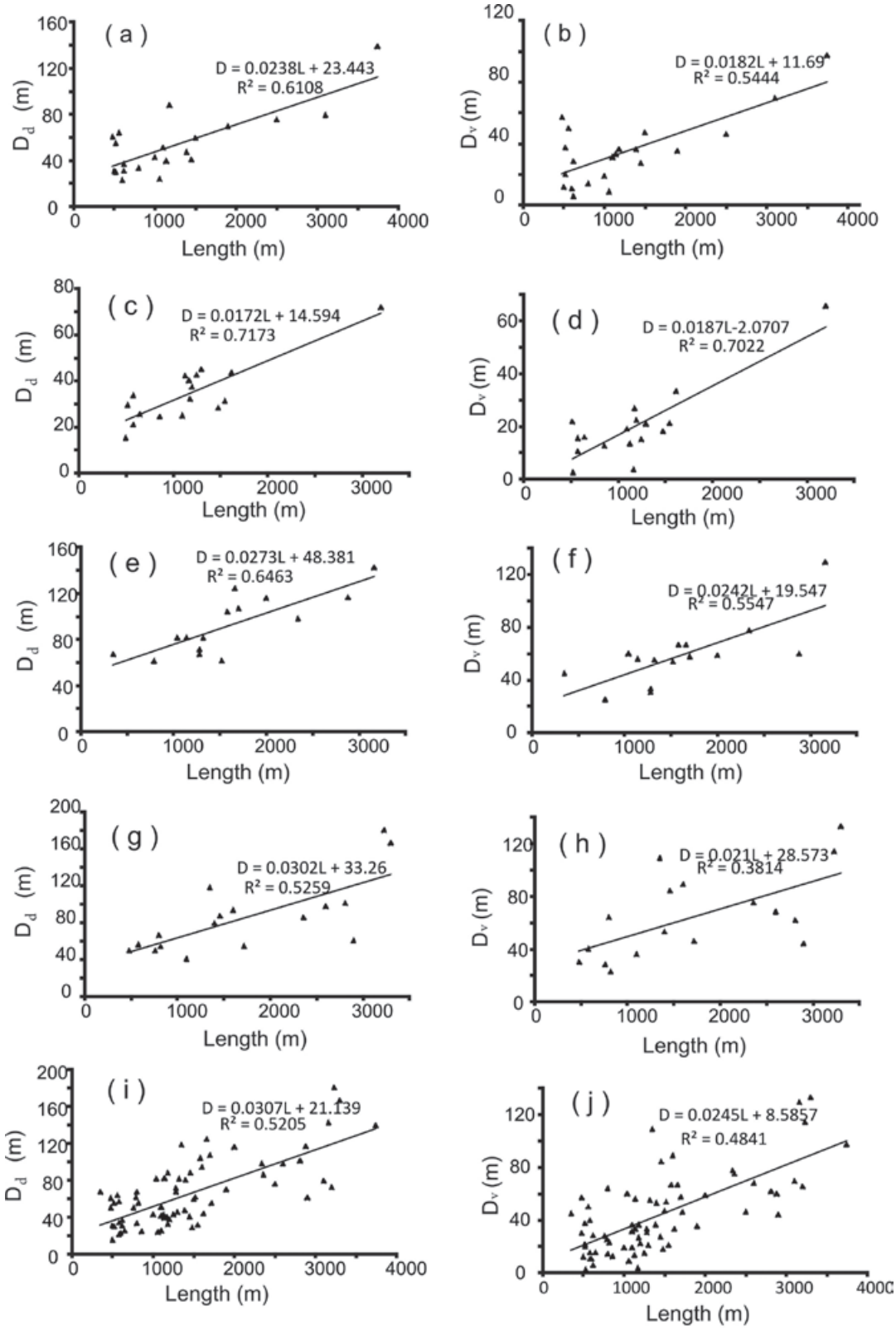

Figure 5. Plots of dip- (D_d) and vertical- (D_v) Displacements versus Length. In (a) – (h), data comes from the two-tip faults of the structural contour maps of T1, T2, T3, and T4, and in (i) and (j) from sum of maps of T1, T2, T3, and T4. In (a), (c), (e), (g) and i, the displacements are the dip-slips (D_d), whereas, in (b), (d), (f), (h) and (j) the displacements are the vertical components (D_v) for the respective levels.

which implies very poor linear relationship between *D* and *L*. The correlation coefficients including all faults are intermediate, showing a moderate linear relationship. Our results are consistent with published data by Tentler and Mazolli (2005), who found that datasets from two-tip faults are better for analysis of *D-L* linear relationship.

Effect of observation level

An isolated fault could be idealized as an elliptical tip line in three dimensions (e.g., Wash and Watterson, 1989; Nicol *et al*., 1996). In that case, when the maximum displacement is measured in the map view, the respective value is only a sub-maximum.

In the study area, we measured data of fault displacement and fault length from four maps (T1, T2, T3, and T4). The results are shown in Figures 7 and 8. The curves of *D-L* ratio in the study area are complicated (Figure 7). The faults generally do not show an ideal ellipse of *D-L* ratio with depth. According to Xu *et al*. (2008), for normal faults the change of *D-L* ratio with depth should be parabolic. Two factors may influence the *D-L* ratio with depth. First, Cowie and Scholz (1992) proposed that

$$\frac{D}{L} = \eta \frac{\sigma_0 - \sigma_f}{\mu} \qquad (2)$$

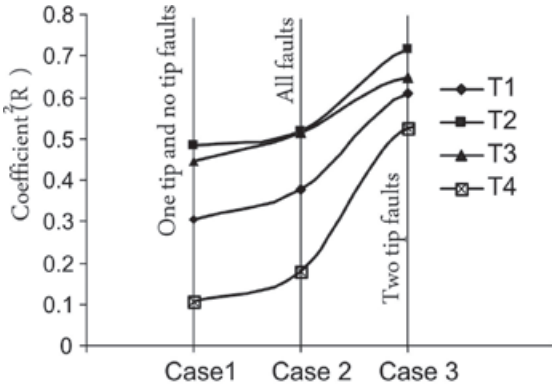

Figure 6. Change of correlation coefficient (R^2) of fault *D-L* relationship for different type of datasets using dip displacement. Case 1 – one-tip and no-tip faults; Case 2 – All faults; Case 3 – Two-tip faults. T1, T2, T3 and T4 are the same as shown in Fig. 2.

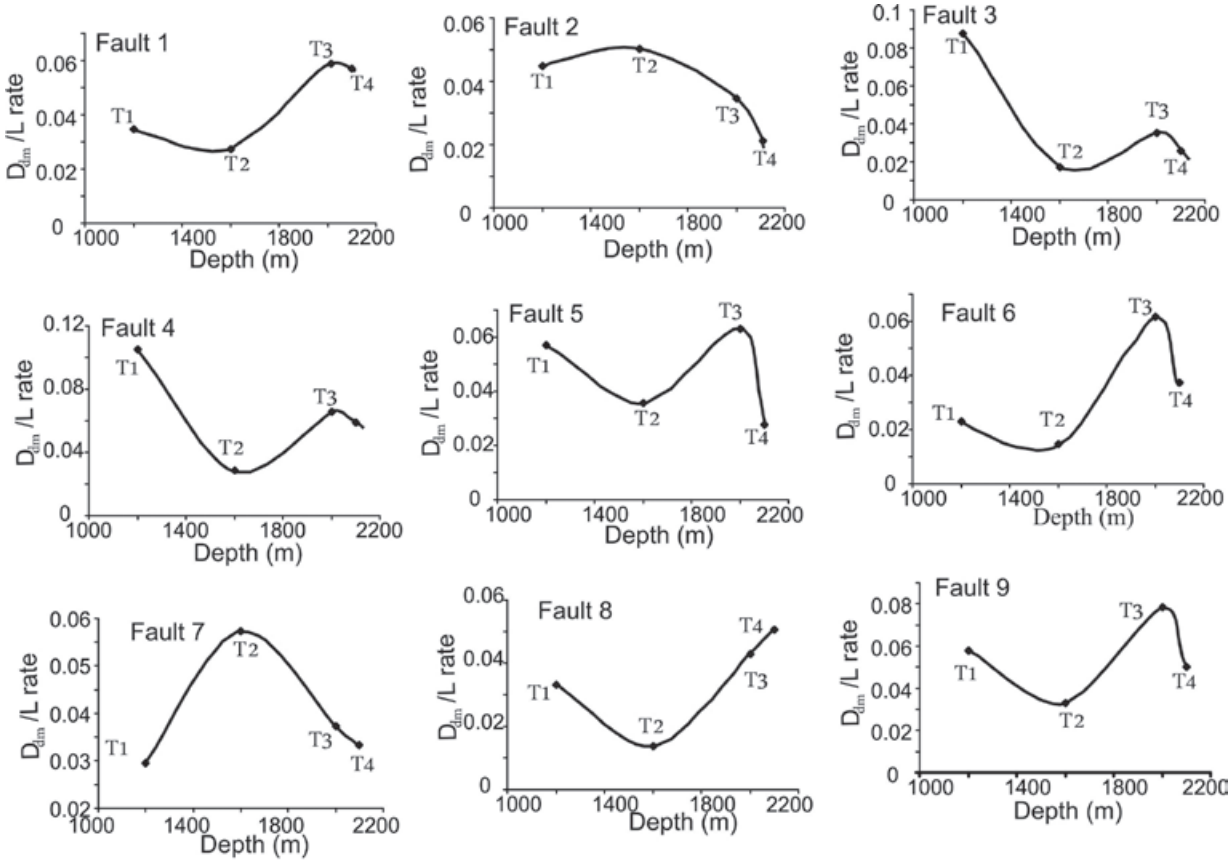

Figure 7. Change with depth of D_{dm} /*L* ratio of 9 faults in the study area. Most faults deviate from the ideal tendency of D_{dm} /*L* ratio of an ellipse. Only fault 2 is consistent with the ideal form of *D*/*L* ratio curve. D_{dm}- maximum dip displacement.

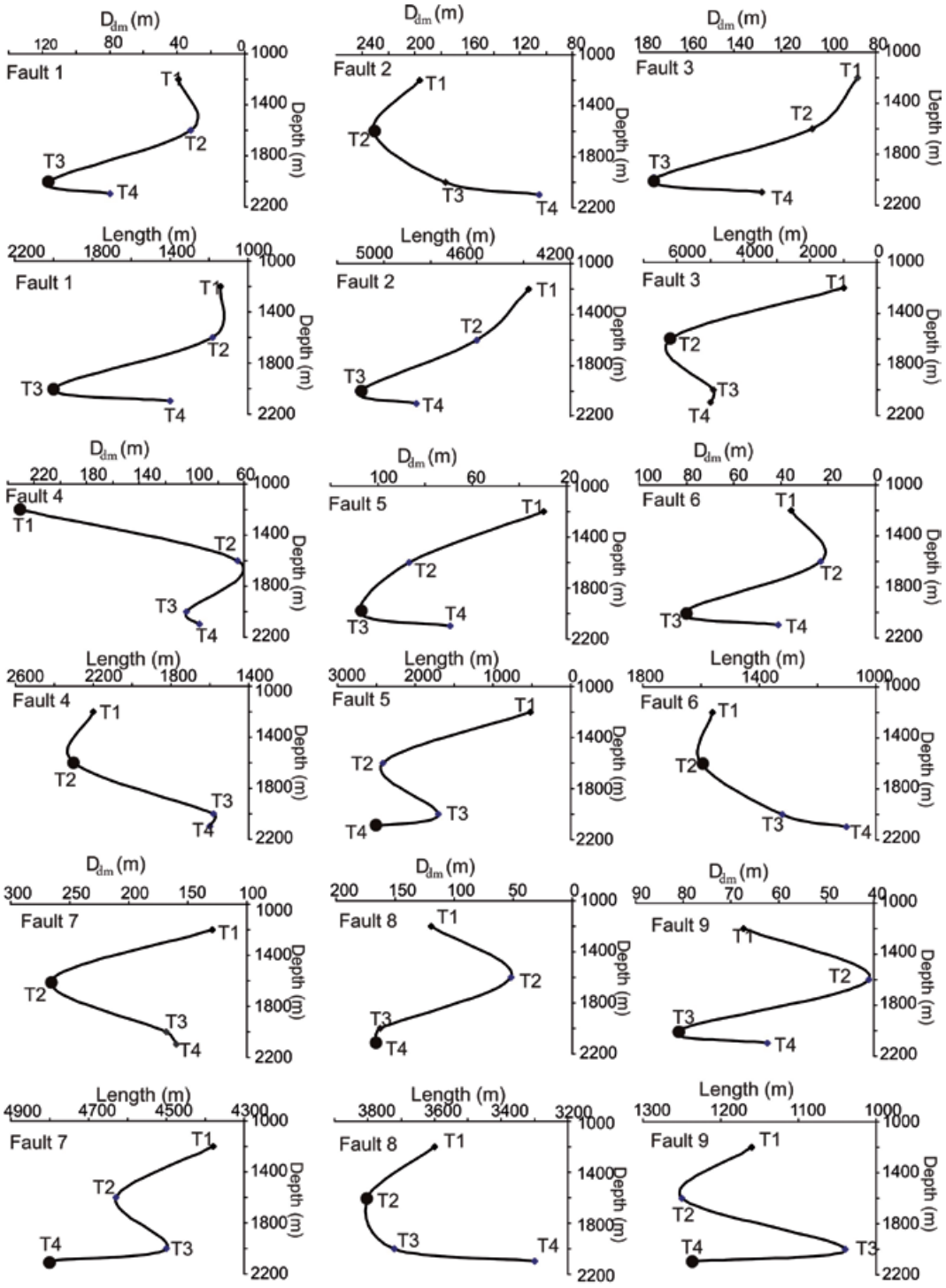

Figure 8. Change of fault displacement and trace length with depth. For most faults, the fault displacement and trace length have not same change tendency. This should influence the *D-L* relationship when *D-L* data are obtained from map views at different levels. D_{dm}- maximum dip displacement.

where σ_0 is the initial yield strength, σ_f the residual frictional strength, μ the shear modulus, and η is a constant. This equation shows that *D-L* relationship is related to the shear modulus, which is dependent on the lithology. The other factors may be the fault linkage in vertical direction. Fault linkage can be observed both in minor faults (Figure 9) and on large faults in seismic cross-sections (see Figure 11 from Mitra *et al*., 2005).

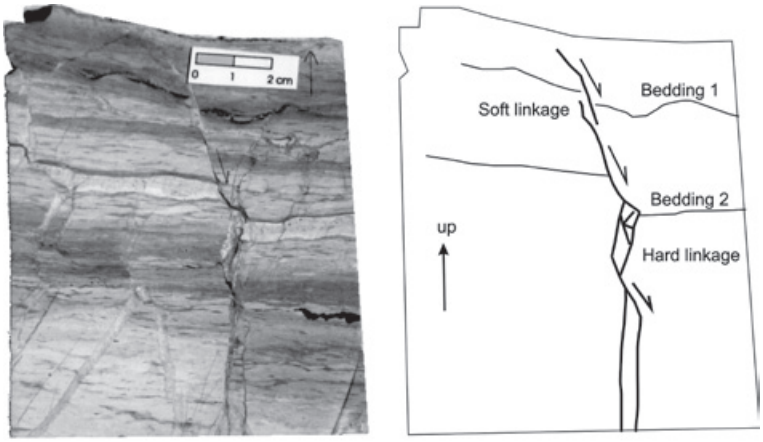

Figure 9. Vertical linkage of minor normal faults observed from the core sample of well 3026D in the Cantarell oilfield.

On the other hand, the change of displacement with depth (observed level) is not the same as that of the fault trace length in most cases (Figure 8). That is to say, the maximum displacement and maximum fault length cannot be obtained at the same observed level. For each observed level, some faults show maximum displacement and maximum length, and other faults do not. Thus faults not showing maximum displacement and maximum length do not represent true *D*/*L* rates. In this way, the *D*-*L* plot cannot show the true relationship between *D* and *L*. The change of displacement with depth (Figure 8) can be considered as a displacement profile in cross-section view. The profiles in figure 8 show irregular but not elliptical forms, which may reflect the vertical fault linkage as well as change of lithology in vertical direction. This will be discussed in the following section.

Discussions

Effect of displacement component

In most published work, normal fault throw is used as a proxy of true displacement to analyze length vs. displacement relationship, or displacement vs. cumulative frequency (e.g., McLeod *et al*., 2000; Meyer *et al*., 2002). This approximation for true total displacement is valid when the lithology is homogeneous, fault dips are high, fault surfaces are not curved, and little fault linkage occurs. Normal faults commonly have dips larger than 60°, which indicates that the vertical component of displacement is about o.86 of dip displacement for pure-dip normal faults. In this way, the vertical component can be approximately used as the true total displacement. Thus it seems reasonable that the coefficients of *D*-*L* linear relationship from vertical displacement are smaller than those from dip displacement in the Cantarell oilfield (Figure 4). Geometrically, three conditions must be met for the dip displacement to be equal to total displacement. First, normal faults should have pure-dip displacement. Figure 10a shows a case in which the fault is oblique-slip. Evidently AF is smaller than GF, where GF is the true displacement and AF is dip displacement. Second, the markers for measuring displacement should be horizontal. In Figure 10a, for the horizontal marker, the dip displacement is AF, whereas for the inclined marker, the dip displacement is EB. As we see, AF is not equal to EB. Third, there is no corrugation of fault surface. If the fault surface is corrugated, the true displacement (CDE in Figure 10b) is generally larger than the dip displacement (AB in Figure 10b).

In our area, most normal faults have a lateral component of displacement (Xu *et al*., 2004). The beddings are not horizontal: dips vary from 10° to 25° (Figure 2c and Figure 3). On the other hand, some faults have a curved surface (Figure 2c, see also the structural cross sections shown in Figure 11 of Mitra *et al*., 2005). All this indicates that there is a deviation of the measured dip displacement from the true displacement in our area. The deviations may be responsible for the lower coefficients of linear regression between dip displacement and length as shown in Figure 4 and Figure 6.

About fault linkage

Fault linkage in this paper is of two kinds (Figure 11). One kind is that two fault segments incorporate and become one single fault by curved propagation or connected fractures around the fault tip area. Two-tip faults are not necessarily isolated faults, because their development history is not known. For example, fault 10 in Figure 3a is a two-tip fault; but the displacement profile of this fault is not symmetric (Figure 12a), which implies that this fault might experience linkage over time. The other kind of fault linkage is that one fault intersects other faults. For this linkage, the stress state around

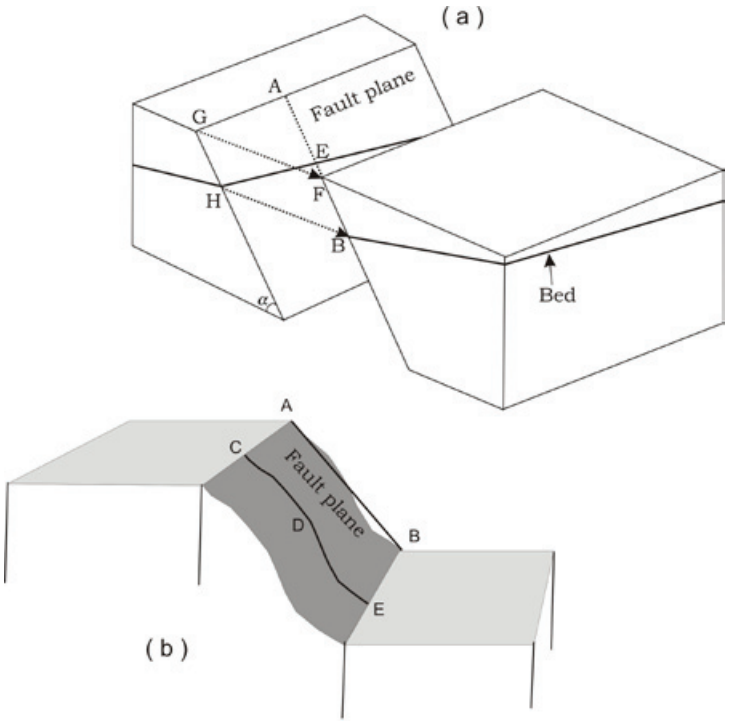

Figure 10. (a) 3D diagram of an oblique fault. See the detailed explanations in text. (b) Corrugated fault for which the true displacement is larger than dip displacement (modified from Lohr *et al*., 2008).

the intersection line is perturbed (Maerten, 2000). In this way, displacement profiles generally exhibit multiple slip maxima near the line of intersection between two faults (e.g., Nicol *et al*., 1996). For the restricted fault in the intersecting fault system, the displacement maximum is located near the intersection line with the restricting fault (Maerten, 2000). This effect is also observed in our area. For example, fault 11 shown in Figure 3a intersects the thrust fault-Sihil fault. The fault gap for fault 11, which is approximately equal to the fault heave, shows a maximum near the intersection line with Sihil fault (fault B) (Figure 12b).

It has been recognized that fault linkage causes the power-law exponent of fault length to decrease in progressive deformation (Cladouhos and Marrett, 1996; Wojtal, 1996). Also, fault linkage may lower the coefficient of power-law population of fault length (Xu *et al*. 2010). This paper displays that the coefficients of D-L relationship decrease for those one-tip o no-tip faults. This is because the fault linkage can cause abrupt increase (incorporated linkage in Figure 11a) o decrease (intersecting linkage in Figure 11b) in fault length.

Effect of lithology and fault reactivation

Besides fault linkage, the lithology of host rocks may influence the development of faults. This effect can be explained by equation (2). Also, anisotropy and heterogeneity such as mechanical layering can cause local stress concentrations and restrict fault formation as pre-existing weakness planes (e.g., Bai *et al*. 2000). In the Cantarell oilfield, layer-parallel slip has been observed (Xu *et al*., 2004). On the other hand, Gudmundsson (2004) proposed that Young's modulus affects fault formation both spatially and temporally. In our area, most measured faults have length larger than the thickness of bedding. Therefore, the mechanics of layering may not influence fault length in the vertical dimension. However, when normal faults intersect the layer-parallel faults, the local displacements will be perturbed near the intersection lines.

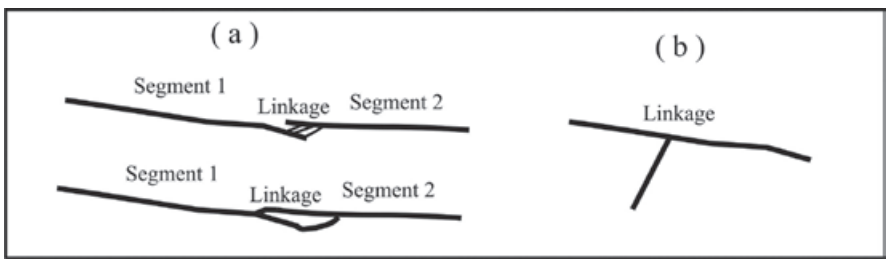

Figure 11. Two ways of fault linkage. (a) Incorporation linkage. (b) Intersecting linkage.

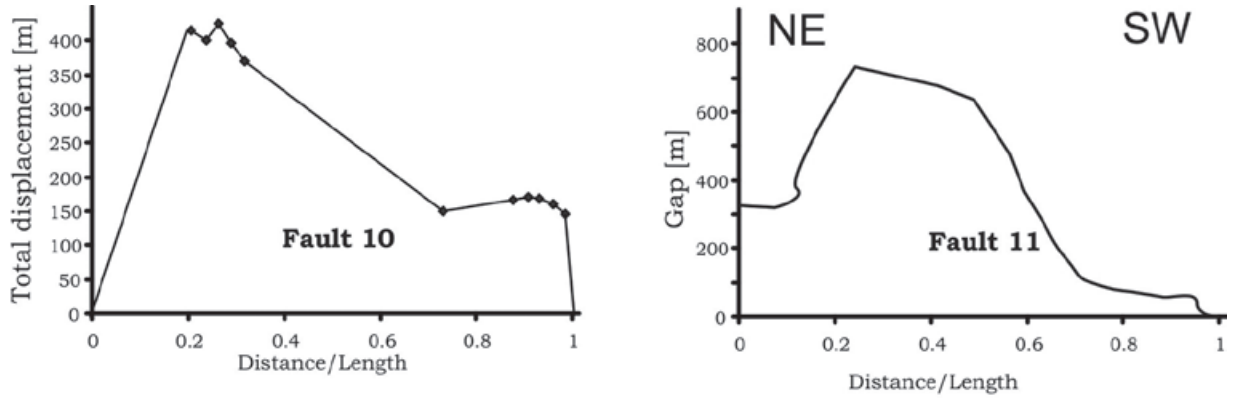

Figure 12. Displacement profile for fault 10 and gap profile for fault 11.

Compression in Miocene in the Cantarell field formed three fault-bounded allochthonous blocks: Akal, Nohoch, and Kutz blocks. These blocks were reactivated in the following extensional episode. In this paper, we mainly studied normal faults in the Akal block, in which most normal faults are new formed faults during last extension (Mitra *et al*., 2005). The thrust faults are not included in our analysis, but some observed normal faults could reactivate reverse faults. The fault shape for normal faults is the same as for reverse faults (Figures 1b, c), therefore, our results of analysis are not affected strongly by fault reactivation.

Conclusions

We investigated three factors which influence the *D-L* relationship from normal faults in the Akal block of Cantarell oilfield in southern Gulf of Mexico. First, from our data the coefficients for linear analysis are larger than those for power-law analysis. In this way, our study supports that a linear relation is the more probable between *D* and *L.* Second, for use studied case the dip displacement of the normal faults is better for analysis of *D-L* relationship. Third, if we select two-tip faults to measure fault maximum displacement and fault trace length, we may obtain linear *D-L* plots with higher correlation coefficients (Figure 6). Finally, the correlation coefficient (R_L^2) for linear *D-L* relationship varies, depending on the observed level, as shown in Figures 7, 8. This is due to maximum displacement and length for all faults not being at a same level.

In general, the data sets from normal faults in the Akal block of Cantarell oilfield suggest that the displacement components, observation levels, and fault linkage can independently influence the relationship between *D* and *L*. Therefore, three aspects should be taken into acount when we analyze the scaling relationships of fault size: The better data could be from the faults with minimum possibility of linkage. The maximum dimensions of all faults should be measured in different levels. Furthermore, the dip displacements may be better than apparent displacements or other displacement components for normal faults, if there is no disturbance of fault linkage and observation level.

Acknowledgement

This work was supported by the project D.01003 of the Instituto Mexicano del Petróleo and the Conacyt projects 049049 and 80142.

Bibliography

Acocella V., Neri M., 2005, Structural features of an active strike-slip fault on the sliding flank of Mt. Etna (Italy). *J. Struct. Geol., 27,* 343-355.

Angeles-Aquino F.J., Reyes-Nuñez J., Quezada-Muñetón J.M., Meneses-Rocha J.J., 1994, Tectonic evolution, structural styles and oil habitat in Campeche sound, Mexico. *GCAGS Trans.* XLIV, 53-62.

Aquino-Lopez J.A., 1999, El Gigante Cantarell: un ejemplo de producción mejorada. Conjunto AMGP/AAPG, Tercera Conferencia Internacional.

Bai T., Pollard D.D., Gao H., 2000, A new explanation for fracture spacing in layered materials. *Nature,* 403, 753–756.

Bonnet E., Bour O., Odlin N.E., Davy P., Main I., Cowie P., Berkowitz B., 2001, Scaling of fracture systems in geological media. *Rev. Geophys., 39,* 347-383.

Caskey S.J., Wesnousky S.G., Zhang P., Slemmons D.B., 1996, Surface faulting of the

1954 Fairview Peak (Ms 7.2) and Dixie Valley (Ms 6.8) earthquakes, Central Nevada. *B. Seismol. Soc. Am., 86,* 761-787.

Childs C., Watterson J., Walsh J.J., 1995, Fault overlap zones within developing normal fault system. *J. Geol. Soc. London, 152,* 535-549.

Cladouhos T.T., Marrett R., 1996, Are fault growth and linkage models consist with power-law distribution of fault lengths. *J. Struct. Geol., 18*, 281-293.

Cowie P.A., Scholz C.H., 1992, Displacement-length scaling relationship for faults: data synthesis and discussion. *J. Struct. Geol., 14,* 1149-1156.

Davis K., Burbank D.W., Fisher D., Wallace S., Nobes D., 2005, Thrust-fault growth and segment linkage in the active Ostler fault zone, New Zealand. *J. Struct. Geol., 27,* 1,528-1,546.

Dawers N.H., Anders M.H., Scholz C.H., 1993, Growth of normal faults: Displacement-length scaling. *Geology, 21,* 1,107-1,110.

Ellis M.A., Dunlap W.J., 1988, Displacement variation along thrust faults: implication for development of large faults. *J. Struct. Geol., 10,* 183-192.

Gudmundsson A., 2004, Effects of Young's modulus on fault displacement. *CR Geosci.,* 336, 85–92.

LeFevre L.V., McNally K.C., 1985, Stress Distribution and Subduction of Aseismic Ridges in the Middle America subduction Zone. *J. Geophys. Res.,* 90, 4,495-4,510.

Lohr T., Krawczyk C., Oncken O., Tanner D., 2008, Evolution of a fault surface from 3D attribute analysis and displacement measurements. *J. Struct. Geol.,* 30, 690-700.

Maerten L., 2000, Variations in slip on intersecting normal faults: implications for paleostress inversion. *J. Geophys. Res.,* 270, 197– 206.

Mansfield C., Cartwright J., 2001, Fault Growth by Linkage: observations and implications from analog models. *J. Struct. Geol., 23,* 745-763.

Marrett R., Allmendinger R.W., 1991, Estimates of strain due to brittle faulting: sampling of fault populations. *J. Struct. Geol., 13,* 735-737.

Mazzoli S., Pierantoni P.P., Borraccini F., Paltrinieri W., Deiana G., 2005, Geometry, segmentation pattern and displacement variations along a major Apennine thrust zone, central Italy. *J. Struct. Geol., 27,* 1,940-1,953.

McLeod A.E., Dawers N.H., Underhill J.R., 2000, The propagation and linkage of normal faults; insights from the Strathspey-Brent-Statfjord fault array, northern North Sea. In: *Processes and controls in the stratigraphic development of extensional basins* 12. Blackwell Science, Oxford, United Kingdom, pp 263-284.

Meyer V., Nicol A., Childs C., Walsh J.J., Watterson J., 2002, Progressive localisation of strain during the evolution of a normal fault population. *J. Struct. Geol.,* 24, 1,215-1,231.

Mitra S., Figueroa G.C., García-Hernández J., Alvarado-Murillo A., 2005, Three-dimensional structural model of the Cantarell and Sihil structures, Campeche Bay, Mexico. *AAPG Bulletin, 89,* 1-26.

Murillo-Muñetón G., Grajales-Nishimura J.M., Cedillo-Pardo E., García-Hernández J., Hernández-García S., 2002, Stratigraphic architecture and sedimentology of the main oil-producing stratigraphic interval at the Cantarell oil field: the K/T boundary sedimentary succession. Society of Petroleum Engineers, *Paper SPE-7431*.

Nicol A., Walsh J.J., Watterson J., Bretan P.G., 1996, Three dimensional geometry and growth of conjugate normal faults. *J. Struct. Geol., 17,* 847-862.

Pacheco A.C., 2002, Deformación Transpresiva Miocénica y el desarrollo de sistemas de fracturas en la porción nororiental de la Sonda de Campeche: Universidad Nacional Autónoma de México, Colegio de Ciencias y Humanidades, Posgrado en Ciencias de la Tierra (Master's thesis), 19-85.

Peacock D.C.P., 1991, Displacement and segment linkage in strike slip fault zones. *J. Struct. Geol., 13,* 721-733.

Peacock D.C.P., 2002, Propagation, interaction and linkage in normal fault systems. *Earth Sci. Rev., 58,* 121-142.

PEMEX-Exploración y Producción, 1999. Las Reservas de Hidrocarburos de México. Volumen II: Los principales campos de petróleo y gas de México: PEMEX Report.

Santiago J., Baro A., 1992, Mexico's giant fields, 1978-1988 decade, in M.T. Halbouty, ed., Giant oil and gas fields of the decade 1978-1988. *AAPG Memoir 54,* 73-99.

Schultz R.A., Soliva R., Fossen H., Okubo C.H., Reeves D.M., 2008, Dependence of displacement-length scaling relations for fractures and deformation bands on the volumetric changes across them. *J. Struct. Geol., 30,* 1405-1411.

Soliva R., Benedicto A., 2005, Geometry, scaling relations and spacing of vertically restricted normal faults. *J. Struct. Geol., 27,* 317-325.

Suppe J., Chou J.T., Hook S.C., 1992, Rates of folding and Faulting determined from growth strata, in: McClay, K.R., Ed., Thrust Tectonics: London Chapman and Hall, 105-121.

Tearpock D.J., Bishchke R.E., 2003, Applied Subsurface Geological Mapping With Structural Methods (2nd Edition). Prentice Hall PTR, 822 p.

Tentler T., Mazzoli S., 2005, Architecture of normal faults in the rift zone of central north Iceland. *J. Struct. Geol., 27,* 1,721-1,739.

Walsh J.J., Watterson J., 1987, Distributions of cumulative displacement and seismic slip on a single normal fault surface. *J. Struct. Geol., 9,* 1,039–1,046.

Walsh J.J., Watterson J., 1988. Analysis of the relationship between displacements and dimensions of faults. *J. Struct. Geol., 10,* 239-247.

Walsh J.J., Watterson J., 1989, Displacement gradients on fault surface. *J. Struct. Geol., 11,* 307-316.

Walsh J.J., Watterson J., 1991, Geometry and kinematic coherence and scale effects in normal fault systems. In: Roberts AM, Yielding, G, Freeman B (eds.), The geometry of normal faults. *Geol. Soc. London Spec. Pub., 56,* 193-203.

Watterson J., 1986, Fault dimensions, displacements and growth. *Pure Appl. Geophys., 124,* 365-373.

Willemse E.J., 1997, Segmented normal faults: Correspondence between three-dimensional mechanical models and field data. *J. Geophys. Res., 102,* 675-672.

Whitman J.M., Harrison C.G.A., Brass G.W., 1983, In: T.W.C. Hilde and S. Uyeda (eds.).Tectonic evolution of the pacific ocean since 74Ma. *Tectonophysics,* 99, 241-249.

Wojtal S.F., 1996, Changes in fault displacement population correlated to linkage between faults. *J. Struct. Geol.,* 18, 265-279.

Xu S-S., D. Li and C. Wen, 1998. Fault characteristics of Nanyang depression. *Explor. Geosci., 13,* 94-99.

Xu S-S., Velasquillo-Martinez L.G., Grajales-Nishimura J.M., Murillo-Muñetón G., García-Hernández J., Nieto-Samaniego A.F., 2004, Determination of fault slip components using subsurface structural contours: methods and examples. *J. Petrol. Geol., 27,* 277-298.

Xu S-S., Nieto-Samaniego A.F., Alaniz-Álvarez S.A., Velasquillo-Martinez L.G., 2006, Effect of sampling and linkage on fault length and length-displacement relationship. *Int. J. Earth. Sci., 95,* 841-852.

Xu S-S., Nieto-Samaniego A.F., Alaniz-Álvarez S.A., Grajales-Nishimura J.M., 2008, Evolution of the geometry of normal faults in the Oligocene volcanic field of the Mesa Central, Mexico. *Boletín de la Sociedad Geológica Mexicana,* 60 (1), 71-82.

Xu S-S., Nieto-Samaniego A.F., Alaniz-Álvarez S.A., Velasquillo-Martínez L.G., Grajales-Nishimura J.M., Murillo-Muñetón G., 2010, Changes in fault length population due to fault linkage. *J. Geodyn.,* 49, 24-30.